Multiple phase transitions may hold the balance between function and disease in cellular bodies

Krishna Shrinivas*
Department of Chemical Engineering, MIT
Institute of Medical Engineering Science, MIT
(Dated: May 19, 2017)

We begin this article by briefly reviewing recent experimental observations of phase transition mediated regulation in biological systems, and their misappropriation in diseased states. Based on experimental evidence, we postulate that in the context of *in vivo* systems, multiple phase transitions may contribute to biological function. Using a mean-field approach, we briefly motivate how weakly self-interacting homopolymers may undergo a first-order phase transition, also known as liquid-liquid demixing. Subsequently, we review exact lattice descriptions of self-interacting polymers that exhibit continuous, percolation-type *geometrical* phase transitions, without singularities in the thermodynamic free-energy, called a sol-gel transition. In the context of *geometrical* percolation transitions, we highlight the potential of real-space normalization group techniques in elucidating various scaling exponents, in the random limit. We briefly touch upon the generalized problem of site-bond correlated percolation. Finally, we close with speculations on how these transitions go awry in misregulated states, through further phase transitions or formation of quenched states.

I. INTRODUCTION

Eukaryotic cells contain several membrane-less organelles, also referred to as cellular bodies or puncta (Fig 1a), which play a central role in compartmentalizing essential biochemical reactions. These organelles are found in both the cytoplasm and the nucleus, and can exist throughout the lifetime of a cell or form temporary structures which dissolve upon regulatory stimuli. Examples of these organelles include nuclear speckles, nucleolus, Cajal bodies etc. in the nucleus, and stress granules, P-granules, P-bodies etc. in the cytoplasm [1][2][3].

These membrane-less organelles are thought to form through liquid-liquid phase separation(LLPS), mediated through multivalent interactions between constituent molecules, and exhibit classic signatures of liquid droplets i.e. they undergo fission and fusion, deform under shearing stress (Fig 1b), and they show fast internal dynamics. *In vitro* studies of multivalent constituents; RNA + RNA binding constituents [4], cognate ligand-proteins [5], and intrinsically disordered proteins[1], all undergo LLPS.

Further, many such proteins often form gel-like states *in vitro* [6][7] and often mature into fibrillar domains or amyloid fibres under long time scales post LLPS. In diseased states, caused through misregulation or mutations in the constituent proteins, the resultant phase separated body resembles a solid-like structure, lacking any internal dynamics [3][8].

In this article, we briefly review how polymers in solution may undergo multiple types of phase transitions.

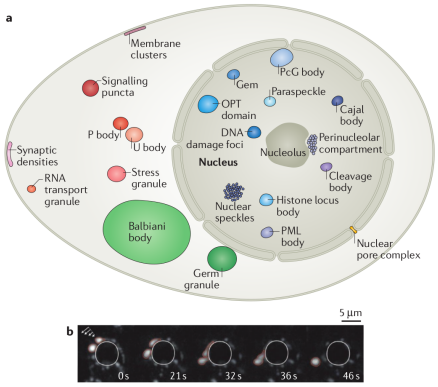

FIG. 1. (a) List of membrane-less organelles inside the eukaryotic cell, formed through phase transitions (b) Typical organelle exhibits features of liquid droplets including shear driven flow and fusion (adapted from [1])

Save for mean-field theories, chain conformational effects will be ignored, and "colloid" like systems will be studies. We will identify critical points and exponents in the lattice framework for the different transitions. Subsequently, we'll explore the role of real-space renormalization group techniques in random percolation and touch on the role of interactions and solvents by looking at generalized correlated site-bond percolation [9]. We'll finally close with speculations in the context of biological systems.

II. LIQUID LIQUID PHASE SEPARATION

Interacting homopolymers in solution can spontaneously phase separate with increasing concentration/ changing interaction strengths. This has been known for a long time [10][11], and the phase diagram mapped out

* krish_s@mit.edu

extensively through Monte-Carlo simulations on finite dimensional lattices [12]. The mean-field hamiltonian of a homopolymer (length N) solution of density ϕ, with effective monomer interaction χ :

$$\beta\mathcal{H} = \frac{\phi}{N} ln(\phi) + (1-\phi) ln(1-\phi) + \chi\phi(1-\phi) \qquad (1)$$

$\chi > 0$ corresponds to "poor solvent" regimes, which is representative of aqueous solvents, and beyond a critical temperature(derived in App A), spontaneous demixing occurs, into polymer "rich" and polmyer "lean" phases. Chain conformation dynamics confound not only the actual location of the transition [13], but introduce several rich crossover phenomena [14] that we won't study, including coil-globule transitions and swelling. We'll briefly point out that multivalent colloids on a lattice (neglecting spatial structure of polymers) provides a *zeroth* order approximation of the system of interest, as biological interactions are short-ranged.

Consider a lattice occupied with colloids of density ϕ with the rest being solvent/voids. If two molecules occupy nearest neighbor positions, they interact with an effective energy ϵ. In class, we have established that the above "lattice gas" grand-canonical system is isomorphic to the canonical Ising model in external field (see [15]). As expected, the liquid-liquid de-mixing mediated by interacting "polymers" can be shown to be a first-order phase transition (order parameter being the local density) in the same universality class of the Ising model (see App A). Detailed Monte Carlo simulations of polymers on a lattice[12], with explicit consideration of chain conformational entropy, show the same results.

III. SOL-GEL TRANSITION

Multivalent polymers which form physical or chemical (reversible or irreversible) cross-links with each other can undergo a phase transition, upon which a macromolecular size cluster is formed. In principle, one may liken this to a "percolation-class" transition, where in, upon the phase transition, a spanning cluster is formed across the entire lattice. We'll begin by applying the mean-field percolation approach to the gelation transition, and review renormalization techinques for non-mean field limits, approximating our proteins as multivalent blobs.

A. Mean-field gelation

In the mean-field model, multivalent colloids (which are our proxy for the proteins) have a valency of f per particle. The system is modeled on the Bethe lattice with each node (site) having $f-1$ neighbors, as depicted in Fig 2. The only allowed structures of cross-linked colloids are

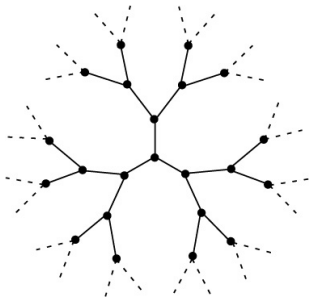

FIG. 2. Bethe lattice with f=3

"tree-like" structures, which don't have any loops, implying that any spanning cluster of n colloids has $n-1$ bonds. Before launching into the details, it is easy to figure out the percolation threshold. Since the Bethe lattice has a fractal "tree-like" structure, for a bond to percolate to the entire system, it is essential for any derived node, the bond percolates to atleast one of it's $(f-1)$ neighbours (See Fig 2). This automatically gives (in agreement with [9]) the threshold (see [16] for an analogy and [17] for comments on cycles or loops of bonds) as:

$$p_c = \frac{1}{f-1} \qquad (2)$$

We begin by drawing a parallel between the order parameter and "thermodynamic" quantities in gelation and other critical phenomena. The natural choice of order parameter for this system is the fraction of colloids connected to the infinite cluster, or gel fraction ϕ_{gel}. The role of temperature in magnets is played by the probability of bond formation p (with an important analogy, see [18]), which has a critical threshold p_c. The distribution of cluster sizes is defined as $n_s(p)$ i.e. the probability that a node is the root of a cluster of size s (for expanded analogy, see [19]) Since the total number of particles is conserved (and equal to N, say) $\sum_s n_s(p)s = 1\ \forall p$. Knowledge of $n_s(p)$ allows us to derive all scaling exponents of interest gelation. Whilst the authors have gone through laborious combinatorics (following [20]), a far simpler argument sheds light on this entire problem. To derive $n_s(p)$, let us make the following observations:

1. All linked clusters of size s have $s-1$ bonds (tree), and remaining $((f-1)s-(s-1))$ are empty.

2. Since n_s is the probability of the root node, there is a degeneracy factor of $\frac{1}{s}$ involved to choose the root node. The root node also has an additional bond which must not be cross-linked (see Fig 2), and since unreacted bonds are indistinguishable, a multiplication factor of $\frac{1-p}{(f-2)s+2}$ is required.

From the two above factors, and noting the entropy of choosing the occupied (and empty) bonds, we can derive:

$$n_s(p) = \frac{1}{s}\frac{1-p}{(f-2)s+2}\binom{(f-1)s}{(s-1)}p^{s-1}(1-p)^{(f-2)s+1} \tag{3}$$

Taking the Stirling's approximation for $s! \approx s^s e^{-s}$, and expanding p around $p_c = \frac{1}{f-1}$, we note the following:

1. Root degeneracy gives a factor of s^{-1}, factorial terms ($s \gg 1$) give an additional factor of s^{-1}.
2. Expansion of the probabilities (around $p_c = \frac{1}{f-1}$) gives a factor of $s^{-0.5}$, and $e^{-(p-p_c)^2 s}$. i.e. Binomial tends to the Gaussian with variance $\propto$ cluster size.

$$\implies n_s(p) \sim s^{-\frac{5}{2}} e^{-(p-p_c)^2 s} \sim s^{-\tau} e^{-\frac{s}{s_\zeta}} \tag{4}$$

Here, drawing an analogy to the Ising system, s_ζ is defined as the correlation cluster size, and we can see that $s_\zeta \sim |p-p_c|^{-\frac{1}{\sigma}}$ where $\tau = \frac{5}{2}, \sigma = \frac{1}{2}$. All scaling exponents can be derived from the above formalism, noting the following

1. Order parameter is $\phi_g(p, s=\infty) = 1 - \sum_{s=1} s n_s(p)$. Gel fraction is 0 below p_c and increases linearly with deviations from p_c in the gel phase.
2. The weight-average degree of polymerization (similar to magnetic susceptibility) is defined as:

$$DP_w = \frac{\sum_s s^2 n_s(p)}{\sum_s s n_s(p)}$$

We can derive the classical exponents from (4) as $\beta = \frac{\tau-2}{\sigma} = 1, \gamma = \frac{3-\tau}{\sigma} = 1, \delta = \frac{1}{\tau-2} = 2$ and $\nu = \frac{1}{2}, \alpha = -1$. Note that, unlike the magnetic $\beta = \frac{1}{2}$, the gelation exponents fall into a different class, the same universality as percolation. It is possible to derive other exponents to shed light on this purely *geometrical* transition, and explicit consideration in the grand canonical ensemble ([21]) can establish that the thermodynamic free energy does not become singular across this transition. The upper critical dimensionality (if hyperscaling where to be obeyed i.e. $d_c\nu = 2 - \alpha$) is found as $d_u = 6$ and lower $d_l = 1$. Hence, the above exponents may not reflect reality in $1 < d < 6$. Whilst exact solutions of the above model are impossible on finite dimensional lattices (other than 2D square lattice), we'll briefly explore some real-space renormalization techniques.

B. Real space renormalization: Lattices

An intuitive, controlled, yet not easily scalable renormalization technique involves understanding the percolation problem through the "cluster-RG" type approach.

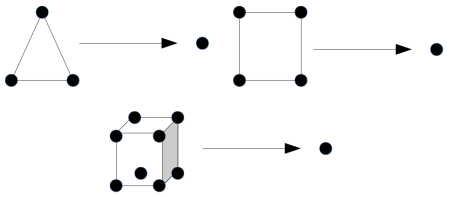

FIG. 3. Cell to site renormalization shown for (a) Triangular 2-D lattice (b) Square 2-D lattice (c) Cubic 3-D lattice

We'll illustrate calculation of this technique using the site percolation approach (see footnote [22] for bond-site duality). Renormalize the sub-lattices so as to change the correlation length by a factor of b i.e. $\zeta' = \frac{\zeta}{b}$. This renormalization group for the percolation probability can be written as (in general, with an external field):

$$\begin{aligned} p' &= \mathcal{R}(p,h) \\ h' &= h\mathcal{R}_2(p,h) \end{aligned} \tag{5}$$

Generally, in absence of external field, $\mathcal{R}(p, h=0) = \mathcal{R}(p) = p$ has three fixed points. The stable supercritical ($p = 1$) and sub-critical points ($p = 0$), as well as the unstable, phase transition point ($p = p_c$). It is easy to derive (details in footnote [23]) the associated thermal exponent. Using a "ghost" approach ([24]), it is also possible to obtain an estimate of y_h, though the author did not pursue this technique. The guiding principle is that when we renormalize a cell to a site, we must develop rules for when the cell is considered "occupied". Potential strategies include; (a) initial cell is spanned in a particular direction (b) initial cell spans in any of one directions (c) initial cell spannable in all directions, and many others. As an illustration (see Fig 3), let us consider writing down the different laws assuming that the decimated site is "occupied" only if the original cluster spans in atleast one (b type) direction:

$$\begin{aligned} &\mathcal{R}_p^{2D\Delta} = p^3 + 3p^2(1-p) \\ &\mathcal{R}_p^{2D\square} = p^4 + 4p^3(1-p) + 4p^2(1-p)^2 \\ &\mathcal{R}_p^{3D\square} = p^8 + 8p^7(1-p) + 28p^6(1-p)^2 + 48p^5(1-p)^3 + \\ &44p^4(1-p)^4 + 24p^3(1-p)^5 + 12p^2(1-p)^6 \end{aligned} \tag{6}$$

For 2-D lattices, it is easy to see that if two sites out of three are occupied, then on can span the triangular lattice, and if greater than 2 sites (which are not in opposite diagonals) are occupied for square lattice, we can span the square cell. For the 3-D cube, the paths were generated using MATLAB (see appendix B). A list of critical points and $\nu = \frac{1}{y_p}$ are generated, as shown in Table I.

Intriguingly, the results for the triangular lattice are nearly exact. However, single cell RG results don't hold up too well for the square sub-lattice in 2 or 3-D

Lattice	$p_{c.RG}$	$p_{c,actual}$	ν_{RG}	ν_{actual}
2D-Δ	0.5	$\frac{1}{2}$	1.354	$\frac{4}{3}$
2D-$\square$	0.39	0.59	1.59	$\frac{4}{3}$
3D-$\square$	0.147	0.31	1.77	0.82
2D-$\square$ (span 1-Direction)	0.618	0.59	1.63	$\frac{4}{3}$

TABLE I. Comparison of single-cell RG predictions to actual (computational) solved exponents and thresholds. Analytic actual results were presented as fractions and Monte-Carlo derived ones with decimal representations

(interestingly the p_c estimate is very close for a different choice of $\mathcal{R}(p)$, see [25] for details). Extensions of this method involve looking at "larger" cells, which perform better [24], but the authors did not have sufficient time to formulate these simulations. The authors close this section by noting that critical exponents for percolation have been exactly solved in 2-D through conformal invariance and Monte Carlo simulations in 3-D [26],[27].

Despite this wealth of information on mean-field, and finite-dimensional percolation models, experimental studies of gelation disagree on static exponents [28][29][30]. A recent study [28] even reported a cross-over in exponents with changing concentration. Several other studies of kinetic gelation [31],[32][33] predict unique, different universality classes for the gelation transition, motivated by Smoluchoswki type coagulation models or mode-coupling theories. Yet other studies [29][34] find that numerical experiments match critical exponents of the percolation class, but intriguingly ones in $d = 4$. Finally, theories of colloidal gelation [35][36] show that multivalent colloids may undergo either gelation type or glassy transitions, with kinetic arrest.

Most interestingly, almost *all* (referenced) studies have explicitly considered irreversible gelation. In the biological context, if gelation is driven, it is definitely through multiple, but weak, reversible interactions [1]. Further confounding occurs due to conformational effects, although Rouse models based on the percolation universality class (largely independent of d) [29][37] seem to agree loosely with experiments. The author is aware that there are numerous approaches listed above for irreversible gelation, which have some degree of overlap, but to his knowledge, the phase transition behavior for reversible gelation of branched polymers continues to evade complete classification.

IV. MULTIPLE TRANSITIONS

We (Sec II,III) have shown that multivalent colloids/polymers can undergo two different type of phase transitions, belonging to different universality classes. In site or bond percolation, if sites (bonds) are fixed, then bonds (sites) percolate randomly. However for the general case, we might envision that both sites and bonds may be vacant (to account for excluded volume or solvent effects), and their interactions correlated through an underlying Hamiltonian (see footnote [38] for distinction from the lattice gas). Whilst the authors do not show the lengthy calculations from [39], to close this article, they borrow a picture from their results on the Bethe lattice [9]. In general, when lattice-gas type interactions are included, both gelation-type and coexistence/phase separation may occur, as illustrated in Fig 4.

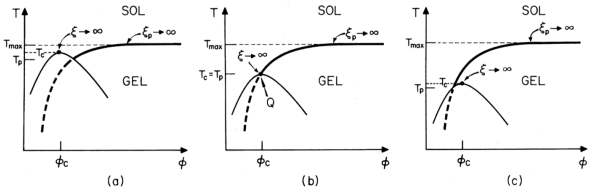

FIG. 4. Phase diagrams for different solvent-monomer interactions, borrowed from [9]. (a) represents a case where two sol phases can coexist without gelation and (c) is vice versa, where gelation precedes or accompanies all phase separation. (b) corresponds to singular case when both co-incide.

A key point to note is that different correlation lengths ζ (thermal) and ζ_p (connectivity) diverge typically at different points, and belong to different universality classes. As illustrated in Fig 4, it is possible to phase separate without gelation (sub-panel a), which would typically correspond to "poor" solvent conditions, and exhibit two kinds of gel phases in "good" solvent conditions (sub-panel c).

V. DISCUSSION

Over the last few years, the import of phase transitions in mediating biological function has been firmly established, in several *in vitro* and *in vivo* studies, reviewed extensively in [1][40][3]. As we have studied above, it is quite obvious that multivalent proteins may show rich phase behavior, exhibiting multiple transitions in different universality classes. Phase separation(LLPS) has been primarily used for marking the presence of such bodies *in vivo* [1][40]. In few studies, like [41], the authors have shown that multivalent proteins and cognate pairs phase separate into liquid bubbles, and this transition also bears several hall marks of the sol-gel transition (more details in Fig 5,Appendix C). Formation of reversible gels without phase separation also potentially mediates biological function, as is observed in the case of nephrin like assemblies (unpublished observations, communicated by Dr. Michael K. Rosen). However, what remains standing is that most studies usually don't probe the mechanistic driving forces of these multiple phase transitions, in the context of critical phenomena.

A common feature of several proteins, especially intrinsically disordered proteins, and RNA that drive *in vivo* phase separation is the presence of multiple aromatic, hydrophobic interactions. This seems to suggest a "poor solvent" *in vivo* condition, and presumably drives phase separation without extensive gelation (a la Fig 4a). Even if sol-gel transitions occur, they might correspond to weakly "quenched" or gelled states close to the percolation threshold. A hallmark of diseased states is their ability to increase interactions through valency [3], or mutations which affect binding affinity [8], which lead to fibrillar or solid like aggregated states (see Fig 6, App C). WT proteins which are implicated in *in vivo* phase separation also aggregate/gel/fibrillate on long time scales (See Fig7, App C).

The above facts allow for an attractive speculation that biological function may be regulated through these (possibly) multiple phase transitions. A principal commonality to most phenomena [5] is the rapid response to stimuli for assembly/disassembly of phases, which enable function. As we have seen in Sec IV, gelation and phase transition are intertwined for multivalent polymers. In order for this rapid switch between two sides of the transition (s) under normal states, the relevant interactions must be tuned relatively close to the threshold(s), lest the system fall too deeply on either side of the critical point(s). This is further supported by the fact that many *in vivo* shifts between the ordered/disordered phases are typically mediated through modification (phosphorylation,acetylation etc) marks on proteins which are written in response to stimuli [1] and reversed(dephosphorylated, deacetylated etc) otherwise, akin to modulating valency, of weak interactions. The advantages of such a mechanism are numerous, of which a key few include:

1. Phase transitions are cooperative, which enables a sharp, switch-like response to stimuli.

2. Phase separation, in particular, allows for formation of a distinct chemical environment which localizes certain biochemical interactions essential for specific functions.

3. The presence of dynamics and rearrangement within weak gels and liquid droplets allows for exchange with environment, in relevant biological time scales.

Abnormal mutations or misregulation of enzymes (which show similar characteristics as long time WT proteins *in vivo*) often change the valency (or effective binding strength) significantly [3],[8],[42][43][44], driving the demixing and gelation too deeply into the phase. This can lead to formation of kinetically arrested gels [35], glassy states [32], or due to the high local concentration, even nucleate precipitation or aggregation of fibers or amorphous protein phases. In fact, in the case of Huntington's disease, which is known to be driven by expansion in CAG repeats of protein Huntington, there exists a strong correlation between increasing repeats (valency) and early onset of disease [45], which is linked with the increasing ability to oligomerize [46], leading to formation of aggregrated bodies.

Further work on uncovering critical exponents and characterizing the phase transitions which mediate biological function *in vivo* is essential to understand the underlying mechanisms better. Viscoelastic and microrheological experiments which are appropriately tweaked may be used to probe these phenomena in *in vitro* assemblies which phase separate and are being explored (private communication, Dr. Michael K. Rosen). Theoretical work on reversible, polymer gelation would shed more light on the interplay b/w gelation and phase separation. Renormalization group techniques which look at dynamics of reversible assembly would be invaluable. Finally, mechanistic understanding of the underlying properties of phase transition mediated biological function will help guide strategies to combat diseased and misregulated states.

VI. ACKNOWLEDGMENTS

The author would like to express his sincere gratitude to Dr. Mehran Kardar, for his thought provoking and fundamental lectures, both in 8.333 and 8.334. They have helped the author immensely in learning to approach his research, and more generally, thinking about science. The author is grateful to Dr. Arup K. Chakraborty for insightful conversations, especially on the broader implications of phase transition mediated function. The author appreciates many stimulating conversations with Dr. Phillip A. Sharp, Dr. Richard A. Young, Dr. Denes Hnisz, Dr. Ben Sabari, Dr. Michael K. Rosen, Dr. Arjun Narayan and Dr. Salman Banani.

[1] S. F. Banani, H. O. Lee, A. A. Hyman, and M. K. Rosen, Nature Reviews. Molecular Cell Biology **18**, 285 (2017).

[2] S. Banjade, Q. Wu, A. Mittal, W. B. Peeples, R. V. Pappu, and M. K. Rosen, Proceedings of the National Academy of Sciences of the United States of America **112**, E6426 (2015).

[3] L.-P. Bergeron-Sandoval, N. Safaee, and S. W. Michnick, Cell **165**, 1067 (2016).

[4] Y. Lin, D. S. W. Protter, M. K. Rosen, and R. Parker, Molecular cell **60**, 208 (2015).

[5] S. F. Banani, A. M. Rice, W. B. Peeples, Y. Lin, S. Jain, R. Parker, and M. K. Rosen, Cell **166**, 651 (2016).

[6] M. Kato, T. Han, S. Xie, K. Shi, X. Du, L. Wu, H. Mirzaei, E. Goldsmith, J. Longgood, J. Pei, N. Grishin, D. Frantz, J. Schneider, S. Chen, L. Li, M. Sawaya, D. Eisenberg, R. Tycko, and S. McKnight, Cell **149**, 753 (2012).

[7] T. Han, M. Kato, S. Xie, L. Wu, H. Mirzaei, J. Pei, M. Chen, Y. Xie, J. Allen, G. Xiao, and S. McKnight, Cell **149**, 768 (2012).

[8] A. Patel, H. Lee, L. Jawerth, S. Maharana, M. Jahnel, M. Hein, S. Stoynov, J. Mahamid, S. Saha, T. Franzmann, A. Pozniakovski, I. Poser, N. Maghelli, L. Royer, M. Weigert, E. Myers, S. Grill, D. Drechsel, A. Hyman, and S. Alberti, Cell **162**, 1066 (2015).

[9] A. Coniglio, H. E. Stanley, and W. Klein, Physical Review Letters **42**, 518 (1979).

[10] P. J. Flory, The Journal of Chemical Physics **10**, 51 (1942).

[11] M. L. Huggins, The Journal of Chemical Physics **9**, 440 (1941).

[12] K. Kremer and K. Binder, Computer Physics Reports **7**, 259 (1988).

[13] A. Sariban and K. Binder, Macromolecules **21**, 711 (1988).

[14] P.-G. De Gennes and T. A. Witten, *Scaling concepts in polymer physics* (AIP, 1980).

[15] Test1, Problem 3.

[16] Note that this definition of gelation renders this problem isomorphic to a branching process, used to model evolution [47].

[17] In real gelation, however, spatial correlations b/w sites tend to induce "cyclical" bond formation, which leads to loops. Further, surface effects, we which wrongly ignore in the Bethe lattice, also play a role in influencing the gel point. However, whether it has an impact on the universality class remains answered.

[18] Unlike random percolation, equilibrium value of p is uniquely specified by a function of graph properties (f,N, bond strength etc.) in gelation. However, in principle, we can map out the properties of gelation as a function of p, which is tuned *in vivo* through the valency/bond interaction/concentration. The equilibrium relation is listed as

$$\frac{p}{(1-p)^2} = Nfe^{\delta G_{rxn}}$$

.

[19] Note that this is different from sn_s, which is the probability that a node belongs to a cluster of size s. is At low p (high temperature in ising model), the bonds are unstable and almost all clusters are single colloids. At high p (low temperatures), nearly all the colloids are connected, and thus n_s is peaked at high s values.

[20] W. H. Stockmayer, The Journal of Chemical Physics **11**, 45 (1943).

[21] R. J. Cohen and G. B. Benedek, The Journal of Physical Chemistry **86**, 3696 (1982).

[22] Whilst site percolation and bond percolation show different critical points for the same lattice symmetries, extensive numerical calculations and conformal mapping in 2-D have established that the critical exponents do not depend on whether it is site or bond percolation.

[23] The analog of the thermal exponent (y_t) can be derived as follows:

$$\delta p \sim \frac{\partial p^{'}}{\partial p}|_{p=p_c,h=0} = \frac{\partial \mathcal{R}(p)}{\partial p}|_{p=p_c,h=0} \sim b^{y_p}$$

This implies that the thermal exponent can be easily derived as

$$y_p = \frac{\log \frac{\partial \mathcal{R}(p)}{\partial p}|_{p=p_c,h=0}}{\log b}$$

.

[24] P. J. Reynolds, H. E. Stanley, and W. Klein, Physical Review B **21**, 1223 (1980).

[25] If the choice of $\mathcal{R}(p)$ were so to ensure that the spanning criteria were along a particular direction, either horizontal or vertical, then our choice of renormalization would be:

$$\mathcal{R}_p^{2D\square,1-Direction} = p^4 + 4p^3(1-p) + 2p^2(1-p)^2$$

.

[26] H. Nakanishi and H. E. Stanley, Journal of Physics A: Mathematical and General **14**, 693 (1981).

[27] A. A. Saberi, Physics Reports Recent advances in percolation theory and its applications, **578**, 1 (2015).

[28] D. Kaya, . Pekcan, and Y. Ylmaz, Physical Review E **69**, 016117 (2004).

[29] J. E. Martin, D. Adolf, and J. P. Wilcoxon, Physical Review Letters **61**, 2620 (1988).

[30] J. E. Martin, J. Wilcoxon, and D. Adolf, Physical Review A **36**, 1803 (1987).

[31] H. J. Herrmann, D. P. Landau, and D. Stauffer, Physical Review Letters **49**, 412 (1982).

[32] A. Coniglio, J. J. Arenzon, A. Fierro, and M. Sellitto, The European Physical Journal Special Topics **223**, 2297 (2014).

[33] R. M. Ziff, E. M. Hendriks, and M. H. Ernst, Physical Review Letters **49**, 593 (1982).

[34] Y. Liu and R. B. Pandey, The Journal of Chemical Physics **105**, 825 (1996).

[35] A. de Candia, E. Del Gado, A. Fierro, N. Sator, and A. Coniglio, Physica A: Statistical Mechanics and its Applications **358**, 239 (2005).

[36] E. D. Gado, A. Fierro, L. d. Arcangelis, and A. Coniglio, Physical Review E **69**, 051103 (2004).

[37] T. H. Larsen and E. M. Furst, Physical Review Letters **100**, 146001 (2008).

[38] The lattice gas/Ising framework can be thought of as a site percolation problem, where the sites are correlated through nearest neighbour interactions. However,

the bonds b/w sites always exist irrespective of whether they are occupied or not, unlike the more general treatment.
[39] A. Coniglio, Physical Review B **13**, 2194 (1976).
[40] A. A. Hyman, C. A. Weber, and F. Jlicher, Annual Review of Cell and Developmental Biology **30**, 39 (2014).
[41] P. Li, S. Banjade, H.-C. Cheng, S. Kim, B. Chen, L. Guo, M. Llaguno, J. V. Hollingsworth, D. S. King, S. F. Banani, P. S. Russo, Q.-X. Jiang, B. T. Nixon, and M. K. Rosen, Nature **483**, 336 (2012).
[42] S. Shu, C. Y. Lin, H. H. He, R. M. Witwicki, D. P. Tabassum, J. M. Roberts, M. Janiszewska, S. Jin Huh, Y. Liang, J. Ryan, E. Doherty, H. Mohammed, H. Guo, D. G. Stover, M. B. Ekram, G. Peluffo, J. Brown, C. DSantos, I. E. Krop, D. Dillon, M. McKeown, C. Ott, J. Qi, M. Ni, P. K. Rao, M. Duarte, S.-Y. Wu, C.-M. Chiang, L. Anders, R. A. Young, E. P. Winer, A. Letai, W. T. Barry, J. S. Carroll, H. W. Long, M. Brown, X. Shirley Liu, C. A. Meyer, J. E. Bradner, and K. Polyak, Nature **529**, 413 (2016).
[43] Y. Wang, T. Zhang, N. Kwiatkowski, B. J. Abraham, T. I. Lee, S. Xie, H. Yuzugullu, T. Von, H. Li, Z. Lin, D. G. Stover, E. Lim, Z. C. Wang, J. D. Iglehart, R. A. Young, N. S. Gray, and J. J. Zhao, Cell **163**, 174 (2015).
[44] D. Hnisz, K. Shrinivas, R. A. Young, A. K. Chakraborty, and P. A. Sharp, Cell **169**, 13 (2017).
[45] G. P. Bates, R. Dorsey, J. F. Gusella, M. R. Hayden, C. Kay, B. R. Leavitt, M. Nance, C. A. Ross, R. I. Scahill, R. Wetzel, E. J. Wild, and S. J. Tabrizi, Nature Reviews Disease Primers **1**, 15005 (2015).
[46] Y. Kim, F. Hosp, F. Frottin, H. Ge, M. Mann, M. Hayer-Hartl, and F. U. Hartl, Molecular Cell **63**, 951 (2016).
[47] R. Lyons, The Annals of Probability **18**, 931 (1990).

Appendix A: Flory homopolymers undergo phase separation

In this mean-field hamiltonian (equation 1 for free energy), phase separation occurs when there is a critical interaction strength which allows energetic considerations to balance out entropic ones. Consider the hamiltonian, where ϕ is the concentration of protein:

$$\beta\mathcal{H} = \frac{\phi}{N} ln(\phi) + (1-\phi) ln(1-\phi) + \chi\phi(1-\phi)$$

Differentiating w.r.t ϕ to derive chemical potential, and checking for convexity:

$$\beta\mu = \frac{ln(\phi e)}{N} - ln((1-\phi)e) + \chi\phi(1-\phi)$$

$$\frac{\partial^2 \beta\mathcal{H}}{\partial\phi^2} = \frac{1}{N\phi} + \frac{1}{1-\phi} - 2\chi$$

$$\frac{\partial^3 \beta\mathcal{H}}{\partial\phi^3} = -\frac{1}{N\phi^2} + \frac{1}{(1-\phi)^2}$$

Setting the third derivative to zero separates the regimes below and above which we expect coexistence. In particular, this is found at :

$$\phi_c = \frac{1}{1+\sqrt{N}}, \chi_c = \frac{1}{2} + \frac{1}{N}$$

For values of $\chi > \chi_c$, we expect spontaneous demixing to happen, and the lines of spinodal meta-stability can be derived from setting the second derivative to zero. Note that $\chi \propto \beta \propto \frac{1}{T}$. Expanding near the critical point with $x \propto \sqrt{N}(1 - \frac{\chi_c}{\chi}) \propto \sqrt{N}(1 - \frac{T}{T_c})$, we can see that:

$$\Delta\phi' \propto x^{\frac{1}{2}}$$

Where $\Delta\phi'$ is the difference in density b/w polymer rich and lean phase near the phase transition, derived from the spinodal. As seen above this gives a $\beta = \frac{1}{2}$, and similar calculation places this mean field theory in the universality class as the Ising model.

Appendix B: Cubic lattice shortest-path spanning code

```
%% Number of ways to span a cubic lattice
%%  Efficient ways to do this

n_d = 3;
n_v = 2^(n_d);
s = [1 1 1 2 2 3 3 4 5 5 6 7];
t = [2 4 8 3 7 4 6 5 6 8 7 8];
G = graph(s,t);

plot(G)

for remove_nodes = 1:n_v-1
    nodes_to_remove = combnk(1:8, remove_nodes);
    count_paths(remove_nodes) = length(nodes_to_remove);
    for i=1:length(nodes_to_remove);
        P =rmnode(G, nodes_to_remove(i,:));
        if(min(degree(P))==0)
            count_paths(remove_nodes)= count_paths(remove_nodes)-1;
        end
    end
end

plot(1:1:n_v-1,count_paths)

%Define the basic renormalization group for the hypercubic lattice
p =0:0.001:1;
R = p.^(n_v);
```

```
R_diff = n_v*p.^(n_v-1);
for i=1:length(count_paths)
    R = R + count_paths(i)*p.^(n_v-i)
        .*(1-p).^(i);
    R_diff = R_diff + (n_v-i)*
        count_paths(i)*p.^(n_v-i-1).*(1-p
        ).^(i) - (i)*count_paths(i)*p.^(
        n_v-i).*(1-p).^(i-1);
end
figure;
plot(p,R-p); hold on;
plot(p, R_diff);

%Fixed points
p_fixed=find(abs(R-p)<10^-4);
%Thermal eigen values
y_p = log(R_diff(p_fixed(2)))/log(2);
```

Appendix C: Supplementary Figures

A brief discussion of supplementary figures is given below, showing how diseased and misregulated states mature over time.

1. Phase separation and the sol-gel transition

The authors of [41] constructed various constructs of two cognate proteins, $SH3_n$ and PRM_n, where n is the valency of each chain. As we know, gelation cannot occur for $f < 3$, as $p_c = \frac{1}{f-1}$ is not reachable, and this is observed in Fig 5b (red and green lines, $n = 1, 2$). The characteristic peak in R_g for $n = 3, 4$ represents a sol-gel transition, and is always accompanied by phase separation(as evinced by closed to open circles in Fig 5b). They also observe phase separation at lower concentrations for higher valency, as shown in Fig 5a, where red dots imply phase separation has occurred. Figs 5(c),(d) show the fastest timescale of decay of intensity scattering and cryo-EM structure of the bubbles, which show presence of oligomerized intermediates.

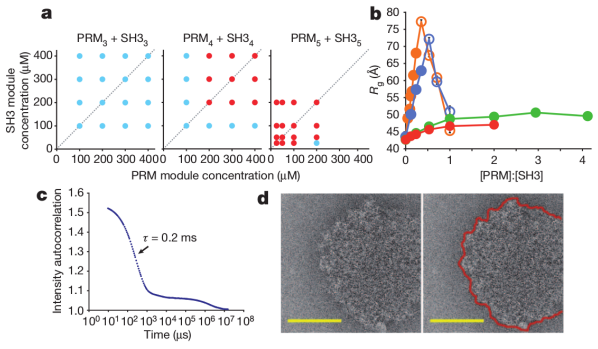

FIG. 5. Phase separation and gelation of SH_n,PRM_n motifs, n is valency or repeats per chain, adapted from [41]

2. Phase separation gone awry

Several studies [5],[40] over the last few years have established that cells dynamically regulate the formation and dissolution of many of these protein-mediated phase separation. Figs 6 reflect that in some diseased states, single mutations which lead to increased valency or abnormally strong bonds led to formation of aggregates with time. Even in WT cells, as shown in Fig 7, some demixed droplets of protein and RNA tend to form gel/-fibres/solidify over time, whereas others do not.

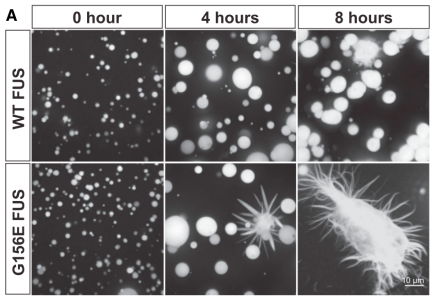

FIG. 6. A recent paper by [8] has shown that mutated FUS proteins, with strong binding interactions, mature from droplets into fibers/aggregates

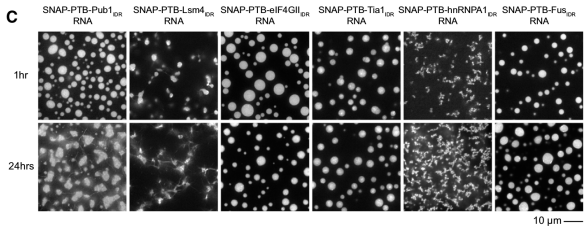

FIG. 7. A recent paper by [4] shows that some phase separated droplets mature over time (24hrs), whilst others remain as reversible droplets, even in WT proteins and RNA